Enthalpy profile of pH-induced flocculation and redispersion of polyacrylic acid-coated nanoparticles in protic ionic liquid, N,N-diethylethanolammonium trifluoromethanesulfonate

Ryo Kanzaki, Mika Sako, Hitoshi Kodamatani, Takashi Tomiyasu, Clément Guibert, Jérôme Fresnais, Véronique Peyre

Journal of Molecular Liquids xxx (xxxx) 118146

Contents lists available at ScienceDirect

Journal of Molecular Liquids

journal homepage: www.elsevier.com/locate/molliq

Enthalpy profile of pH-induced flocculation and redispersion of polyacrylic acid-coated nanoparticles in protic ionic liquid, *N*,*N*-diethylethanolammonium trifluoromethanesulfonate

Ryo Kanzaki [a], Mika Sako [a], Hitoshi Kodamatani [a], Takashi Tomiyasu [a], Clément Guibert [b], Jérôme Fresnais [c], Véronique Peyre [c]

[a] *Graduate School of Science and Engineering, Kagoshima University, 1-21-35, Korimoto, Kagoshima 890-0065, Japan*
[b] *Sorbonne Université, CNRS, Laboratoire de Réactivité de Surface, F-75005 Paris, France*
[c] *Sorbonne Université, CNRS, Laboratoire Physico-Chimie des Electrolytes et des Nanosystèmes Interfaciaux, PHENIX, F-75005 Paris, France*

ARTICLE INFO

Article history:
Received 6 September 2021
Received in revised form 8 November 2021
Accepted 17 November 2021

Keywords:
Nanoparticle
Ionic liquid
Calorimetric titration
Polyacrylic acid
Flocculation

ABSTRACT

Maghemite nanoparticles coated with polyacrylic acid (pAA) were dispersed in the protic ionic liquid, diethylethanolammonium trifluoromethanesulfonate ($DEEAH^+ \cdot TfO^-$), and the thermodynamics of particle dispersion was studied by means of potentiometric and calorimetric titrations over the entire accessible pH range. As previously reported, the domain of colloidal stability is divided into two pH regions, mildly acidic and basic, separated by a flocculation domain at an intermediate pH. In this study, solvent $DEEAH^+ \cdot TfO^-$ was first characterized in terms of the thermodynamic parameters of two reference reactions: autoprotolysis and ionization of acetic acid. A negative autoprotolysis entropy is obtained due to hydrogen-bond formation between the neutralized solvent cation, DEEA, and the neighboring cation $DEEAH^+$. This suggests that the solvent structure is reinforced by the formation of neutral species, being an opposite trend to both ethylammonium nitrate and water. Second, the ionization and flocculation of pAA-coated nanoparticles (CNps) in the ionic liquid were examined. The potentiometric results could be modeled using a simple pAA ionization, independent of the aggregation state over the entire pH range. However, the calorimetric titration detected extra heat generation in an acidic condition prior to flocculation, in addition to an ionization enthalpy of pAA of 30 kJ/mol. This exothermic contribution is attributed to a change in the solvation process of CNps in the ionic liquid. Herein, we propose a model in which different types of solvation in the acidic and basic domains are sufficient to ensure colloidal stability, while aggregation unfolds between the switching pH.

1. Introduction

Electrolytes having a melting point lower than 100 °C are called ionic liquids. Its unique and desirable physico-chemical characteristics such as low vapor pressure, high thermal stability, and a large electrochemical window makes it a potential alternative to molecular solvents. Its feature as an extremely condensed electrolyte solution with no solvent species is also of interest, both for applications and for the development of the hitherto established electrolyte solution theory in the concentrated range.[1–6] This is because the most salts studied as electrolytes in solution so far have a limited solubility, whereas ionic liquids can exist as a solvent containing 100% of ions. In this context, we identified some unique behaviors such as an athermal metal ion-anionic ligand exchange and a concentration-independent ionic activity coefficient.[7,8]

Among the possible uses of ionic liquids as solvents, they can be dispersing media for colloidal dispersions, which have unforeseeable potentialities.[9,10] For colloidal dispersions of charged nanoparticles in water, the addition of electrolytes is generally the primary cause for reduced colloidal stability. In fact, the conventional DLVO theory predicts that the ionic strength decreases monotonically the interparticle repulsion. If this model remained valid in ionic liquids, they could not be "good" dispersing media of colloids because they are considered as extremely concentrated electrolyte solutions. However, stable dispersions of nanoparticles have been obtained in various ionic liquids,[11–23] implying a different stabilization mechanism but electrostatic repulsion. The role of the formation of solvation layers of ions at the surface of the nanoparticles, acting as protective layers, is one possible explanation. The mechanisms underlying the formation of these protective lay-

E-mail address: kanzaki@sci.kagoshima-u.ac.jp

https://doi.org/10.1016/j.molliq.2021.118146
0167-7322/

ers and how they are influenced by the initial charge of the particles and of the nature of the surrounding ionic species are still under debate.

For this aspect, protic ionic liquids, comprising onium salt, are interesting liquids because they act as amphoteric solvents, that is, the dissociable hydrogen ion on the cation makes the liquid able to take part in acid-base reactions, like as water. This property enables the charge of nanoparticles to be varied by the addition of acids or bases in order to modify the degree of ionization of the surface ionizable groups. In our previous studies, we explored maghemite nanoparticles coated with polyacrylic acid (pAA) dispersed in ethylammonium nitrate (EAN).[24] In water, although these pAA-coated nanoparticles (CNps) disperse under neutral and basic conditions, they form irreversible aggregates in acidic solutions. Conversely, CNps can be dispersed in both basic and strongly acidic EAN, and interestingly, they form aggregates at weakly acidic pH that can redisperse when an appropriate pH condition is set again. Similar behavior has been observed in another protic ionic liquid, diethylethanolammonium trifluoromethanesulfonate ($DEEAH^+ \cdot TfO^-$).[25] These observations indicate that the aggregation mechanism in ionic liquids is different from that in water. In the present study, we investigated the thermodynamics of the aggregation process of CNps in $DEEAH^+ \cdot TfO^-$ upon pH variation. Potentiometric and calorimetric titrations were performed, both in water and in the ionic liquid, for comparison. This is the first determination of the enthalpy involved in nanoparticles aggregation in an ionic liquid.

2. Experiments

2.1. Materials

Maghemite nanoparticle synthesis, size-sorting and pAA coating procedures have been described elsewhere.[25] Briefly, γ-Fe_2O_3 nanoparticles were synthesized using Massart's method,[26,27] followed by a size-sorting procedure based on the ionic strength of HNO_3 to reduce size polydispersity.[28,29] Nanoparticles of the fraction of 5 nm in the number mean characterized by DLS (Zetasizer Nano ZS, Malvern) were then coated with pAA (2100 g/mol, Sigma-Aldrich, used as received) by means of the precipitation-redispersion protocol,[30,31] yielding CNps with a size of 9 nm. The CNp content of the aqueous dispersion was 0.99% as Fe_2O_3, determined by the chelatometric titration of iron using EDTA and Cu-PAN,[32] after decomposition by 4 M HCl.

The solvent ionic liquid was synthesized by a neutralization method, as previously described.[25] An aqueous solution of trifluoromethanesulfonic acid (TfOH; Sigma-Aldrich, 99%) was added dropwise into an aqueous solution of *N*,*N*-diethylethanolamine (DEEA; Sigma-Aldrich, 99.5%) in a 0 °C water bath until mildly acidic condition was achieved. Then, the aqueous solution of the onium salt, *N*,*N*-diethylethanolammonium trifluoromethanesulfonate ($DEEAH^+ \cdot TfO^-$), was dried in vacuo for a few weeks at 60 °C to yield a viscous, clear or pale red liquid (hereafter referred to as PIL). The water content was typically 800 ppm, as determined by Karl Fischer titration (APB-620, Kyoto Electronics Manufacturing).

The CNp dispersion in the PIL was obtained by mixing the aqueous dispersion into the same mass of basic PIL containing excess DEEA (i.e., the final content of CNp after removing water is also almost 1% as Fe_2O_3), followed by freeze-drying and subsequent vacuum-drying for a few weeks until the water content of the control (without CNp) becomes less than 1500 ppm (typically, 1000 ppm). Acidic dispersion was obtained by further adding an acidic PIL solution (using TfOH as an acid) with monitoring pH. This dispersion was used for titrations after it was confirmed to be stable for several days. Notably, the direct protocol to achieve acidic dispersions, that is, mixing of the aqueous CNp dispersion and an acidic PIL, causes irreversible precipitation, even when a basic condition is attained by the addition of excess DEEA.

2.2. Measurements

Potentiometric titration was performed using an IS-FET pH electrode (0040-10D, HORIBA) at 25 °C. The output potential of this electrode, *E*, obeys the Nernst equation:

$$E = E_0 + 0.059 \log \frac{[H^+]}{\mathrm{mol\,dm^{-3}}} \quad (1)$$

where E_0 is the formal potential of the IS-FET electrode, determined by separately performed neutralization titration. The fluctuation in *E* was 0.1 mV in the most pH region analyzed, with no drift within the measurement timescale (a few minutes for each titration point), which was maintained even in the turbid solution (CNps are aggregating). The excess proton H^+ actually denotes H_3O^+ in water and TfOH in the PIL, respectively. The degree of dissociation, α, can be obtained as follows.

$$\alpha = 1 - \frac{C_H - [H^+] + \frac{K_{AP}}{[H^+]}}{C_Y} \quad (2)$$

where C_H and C_Y are the total concentrations of H^+ and acetic acid in the sample solution, respectively, and K_{AP} is the autoprotolysis constant. In the case of CNp, the symbol Y denotes the ionizable –COOH group of the surface pAA that can participate in the acid-base equilibria, and the C_Y value was determined from the titration data. Typically, 2 cm^3 of a sample solution containing 0.02 mol dm^{-3} of Y placed in a thermostated glass cell was titrated by 0.05 mol dm^{-3} acidic or basic titrant solution added with an autoburette (APB-410, Kyoto Electronics Manufacturing).

Calorimetric titration was performed with an isoperibol-type lab-made titration calorimeter (based on MPC-11, Tokyo Riko, Japan) at 25 °C. Details of the equipment have been described elsewhere.[8,33] For each titration point, a few tens of mm^3 of titrant was injected over approximately 10–20 s into the sample solution (initial volume: 2.5 cm^3). After the solution is completely mixed, the heat generation stops, and the solution temperature returns to the equilibrium temperature according to Newton's law of cooling (exponential). The heat generated in the injection was determined from the hypothetical adiabatic curve and vessel heat capacity. The vessel heat capacity was determined before and after each titration series by referring to the Joule heat. Since the hypothetical adiabatic curve showed a linear plateau with no anomalous heat and no baseline drift was observed, very slow reactions, such as aggregate growth, are unlikely within the measurement timescale. Typical thermograms, experimental conditions, and precision are found in the Supporting Information (SI).

3. Results and discussion

3.1. CNP dispersion and aggregation in water

3.1.1. Potentiometric titration in water

Prior to investigation in ionic liquids, the behavior of CNp in water, containing 0.1 mol dm^{-3} NaCl as the supporting electrolyte, has to be elucidated. Fig. 1(a) shows the titration curve of CNps dispersed in a neutral aqueous solution with HCl solution as a function of the degree of titration, H/Y; the added amount of H^+ (or HCl) divided by the initial amount of Y. Fig. 1(b) depicts α vs. pH, where pH is defined as $pH = -\log([H^+]/\mathrm{mol\,dm^{-3}})$. The blank symbols indicate that the solution was turbid, which was confirmed via visual observation. As shown, aggregation occurs when pH becomes 3.7, where α is ≈ 0.1. This critical pH value is similar to the previously reported value.[34] Even when aggregation occurred, no drift or fluctuation was observed in emf within the experimental timescale. In our current experiment, the aggregates did not redisperse when the pH was rewound to the initial dispersing condition.

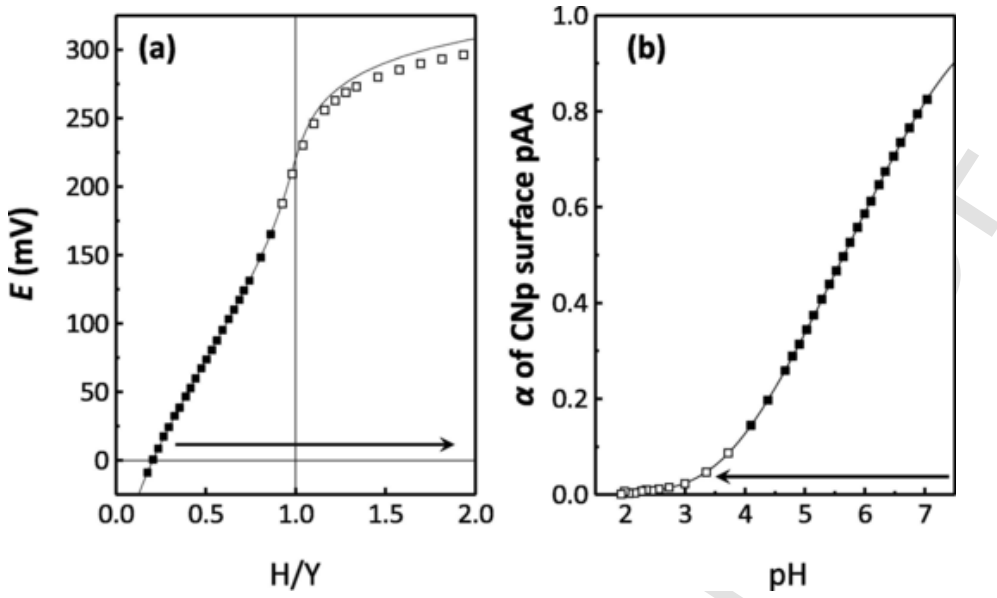

Fig. 1. Potentiometric titration curve of pAA-coated γ-Fe_2O_3 nanoparticles in water, titrated with aqueous HCl solution. (a) IS-FET output potential as a function of H/Y; the total amount of H^+ (from HCl) divided by the amount of ionizable –COOH in pAA. (b) Degree of dissociation of pAA, α, as a function of pH = −log [H^+]/(mol dm^{-3}). Blank symbols exhibit that the solution is turbid (by eyes). Arrows indicate the direction of the titration.

The solid line in Fig. 1 is the theoretical curve using the following equation.

$$\mathrm{pH} - \log \frac{\alpha}{1-\alpha} = \mathrm{p}K_\mathrm{a}{}^0 + \beta\alpha \tag{3}$$

This type of polynomial, proposed and detailed for pAA in water, [35–37] reproduced satisfactorily the ionization equilibrium of the CNp surface both in the dispersing region at high pH and in the aggregating zone, as shown. A slight drop in emf at high H/Y (low pH) may originate from the electrode sensitivity for high H^+ concentration, and is ignorable in α scale. According to least squares fitting, $pK_a{}^0$ = 4.56 and β = 2.19 were obtained. The left side of equation (3) corresponds to the apparent pK_a value of Y at a given pH, $-\log \frac{[H^+][Y]}{[HY]}$, described as $pK_a{}^{app}$ hereafter. Unlike monomer monoacids, this value varies depending on α in the case of CNp. Interestingly, the $pK_a{}^0$ value, which is the extreme value of $pK_a{}^{app}$ when α approaches zero, is close to the pK_a value of acetic acid in water (pK_a = 4.76). This means that the acidity of the carboxylic group on the CNp surface resembles an acetic acid monomer when CNp is uncharged. When α increases, the negative charge on CNp increases, which tends to suppress further dissociation. This results in an increase in the $pK_a{}^{app}$ value. The β value acts as the coefficient of this effect on α. Since coexisting ions in the bulk phase may reduce this electrostatic effect, the β value is expected to decrease with increasing ionic strength. Surprisingly, the β value was much smaller than that in $DEEAH^+ \cdot TfO^-$ (β = 4.8, as described later, or 7.0[25]).

3.1.2. Calorimetric titration in water

In order to investigate the aggregation mechanism in more detail, calorimetric titration was performed. The same CNp sample prepared for the potentiometric titration was used. In Fig. 2(a), the apparent molar reaction enthalpy is plotted in kJ/mol, which is given by the heat of reaction q_r divided by the amount of the titrant (HCl), n_H, as a function of the degree of titration H/Y after each injection. Titration was carried out three times, demonstrating good reproducibility. The shaded area indicates the pH region of aggregation that was formerly observed during potentiometric titration. As expected from the protonation enthalpy of acetate (0.4 kJ/mol, endothermic),[38] as well as the heats of ionization and dilution of pAA,[39,40] the heats of reaction are small, less than 2 kJ/mol throughout, with an endothermic peak at H/Y = 0.5.

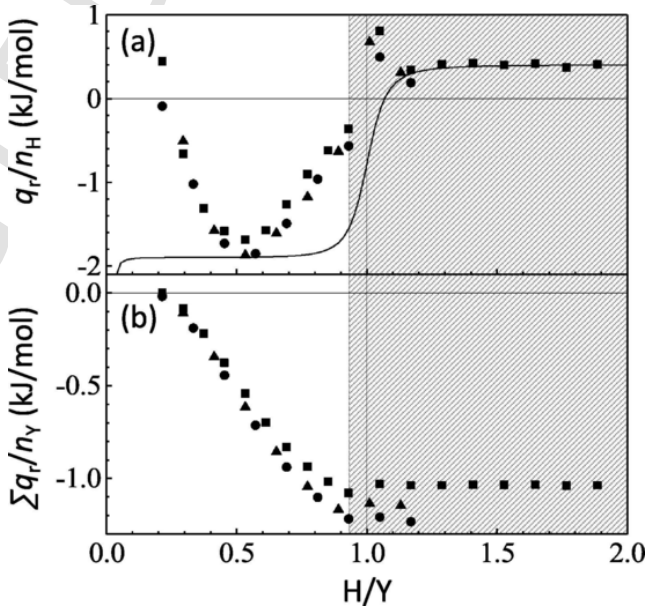

Fig. 2. Calorimetric titration curve of pAA-coated γ-Fe_2O_3 nanoparticles in water titrated with aqueous HCl solution. (a) Heats of reaction (q_r) divided by the amount of H^+ in titrant (n_H). (b) Cumulative heat of reaction, Σq_r, divided by the total amount of Y; ionizable –COOH in pAA. H/Y is the total amount of H^+ divided by that of Y. Shaded area exhibits the H/Y range of forming aggregation that was observed by the potentiometric titration. Symbols represent 3 replicate titrations.

Assuming only protonation processes generate the heat of reaction, q_r at the *i*-th injection (titration point *i*) is written as follows.

$$q_\mathrm{r} = -\Delta H_a^\circ \left(v_i[\mathrm{YH}]_i - v_{i-1}[\mathrm{YH}]_{i-1}\right) + \Delta H_\mathrm{AP}^\circ \left(\frac{v_i K_\mathrm{AP}}{[\mathrm{H}^+]_i} + \frac{v_{i-1} K_\mathrm{AP}}{[\mathrm{H}^+]_{i-1}}\right) \tag{4}$$

where ΔH_a° and ΔH_{AP}° are the enthalpies of ionization of Y and autoprotolysis, respectively, and v_i is the volume of the sample after *i*-th

injection. The solid line in the figure is the calculated q_r curve, where the ionization equilibrium of pAA obeys equation (3) with using potentiometrically obtained pK_a^0 and β values. The small exotherm observed at H/Y > 1.0 was treated as a constant baseline (0.4 kJ/mol). From the minimal value around H/Y = 0.5, ΔH_a° = −2.3 kJ/mol (exothermic ionization) is applied in the first attempt. However, the theoretical curve assuming the above-mentioned model for ionization equilibrium could not reproduce obviously the titration pathway. Since the potentiometric titration curve has been thoroughly explained, processes other than the protonation of the surface pAA are presumed. According to Fig. 1(b), the α value of the CNp surface is more than 0.8 at the beginning of the titration, then decreases to 0.1 before aggregation. The decrease in the pAA net charge will cause a disruption of the electric double layer, along with the breaking down of the hydration structure. In addition, the newly formed hydration structure of the released counterions also contributes to the heat of the reaction. As these heats overlap with the heat of protonation, they are difficult to be separated, resulting in the complicated enthalpy profile. Note that processes with a comparable enthalpy were observed for ionization of pAA [41] and mixing of pAA and a cationic polymer electrolyte [42], so that this calorimetrically caught process is attributed to the change in the solvent structure in the vicinity of pAA or the solvation state. Notably, CNp disperses stably with no significant change in the hydrodynamic diameter (D_H) in this pH region.[26] This indicates that, although the structural charge of the CNp decreases upon titration, which in turn modifies the electric double layer, the effective charge remaining on the CNp is still sufficiently high to ensure stabilization. When H/Y is close to 1, CNp starts aggregating. The slight exotherm at the point of aggregation was observed reproducibly, possibly indicating an exothermic process of aggregation, although the corresponding heat was negligibly small. In order to obtain the overall reaction enthalpy, the cumulative heat of reaction divided by the amount of Y is shown in Fig. 2(b). As shown, a 1.1 ± 0.1 kJ/mol endotherm is obtained. This endotherm is larger than that for the protonation of acetate. The difference of 0.7 kJ/mol in the endotherm could be attributed to the disruption of the electric double layer. A small but positive enthalpy suggests an entropic driving force during this process, plausibly the release of counterions.

3.2. Acid-base property of $DEEAH^+ \cdot TfO^-$

In $DEEAH^+ \cdot TfO^-$, autoprotolysis is described as follows,

$$DEEAH^+ + TfO^- \rightarrow TfOH + DEEA \quad (5a)$$

that corresponds to the autoionization in water.

$$2H_2O \rightarrow H_3O^+ + OH^- \quad (5b)$$

The autoprotolysis constant K_{AP} = [TfOH][DEEA] was formerly determined as pK_{AP} (= −log K_{AP}) = 14.9.[25] This value is related to both the ability of TfOH to release and that of DEEA to accept H^+. In the first step, we will explore their H^+ exchange abilities using acetic acid as a probe. In the second step, we will analyze the entropic and enthalpic contributions to the Gibbs energy of autoprotolysis, in order to gain information as the acid-base reaction medium of the PIL.

3.2.1. Ionization behavior of $DEEAH^+ \cdot TfO^-$ using dissociation constant of acetic acid

Potentiometric titration of acetic acid in the PIL was performed as described previously. Fig. 3 shows the degree of dissociation (α) of acetic acid as a function of pH (−log [TfOH]/mol dm^{-3}). The solid line was calculated using acid dissociation constant of acetic acid in the PIL, pK_a = 11.1, which was obtained by a least-squares procedure. This value is much larger than those in water (4.76) and in EAN (5.45). Basically, it is explained by the stronger acidity (proton donating ability) of TfOH, which is the actual H^+ donor in the PIL, than that of H_3O^+ in water and HNO_3 in EAN. Nevertheless, we here explain the origin of the difference by the solvent basicity, by considering the following reaction.

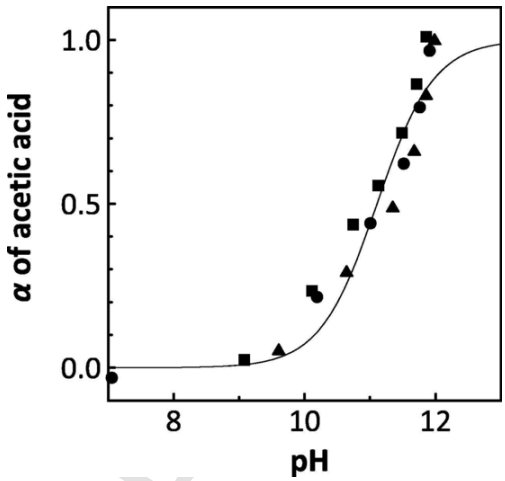

Fig. 3. Potentiometric titration curve of acetic acid in $DEEAH^+ \cdot TfO^-$. Degree of dissociation of acetic acid (α) is plotted as a function of pH = −log [TfOH]/(mol dm^{-3}). Solid curve is the theoretical line using the dissociation constant pK_a = 11.1 (see text). Symbols represent 3 replicate titrations.

$$CH_3COO^- + DEEAH^+ \rightarrow CH_3COOH + DEEA \quad (6)$$

This is reasonable because the acid dissociation of acetic acid occurs in a basic region, according to the autoprotolysis constant of the PIL. The base dissociation constant, pK_b (= −log $[CH_3COOH][DEEA]/[CH_3COO^-] = pK_{AP} - pK_a$), of acetate in the PIL is 3.8, which is slightly smaller than that in EAN (pK_b = 4.41). If acetate is assumed to have the same basicity in these ionic liquids, $DEEAH^+ \cdot TfO^-$ should have a weaker basicity by 0.6 in pK unit than EAN. In contrast, the pK_b value of each base (actual H^+ withdrawer) of respective ionic liquid in aqueous solution is 4.0 (DEEA) and 3.3 (ethylamine), indicating that DEEA has a weaker basicity by 0.7 p*K* units than that of ethylamine. Comparison of these values indicates that the basicity of acetate is practically independent of the solvent in these ionic liquids and water. In turn, the remarkably large pK_a value of acetic acid in the PIL is solely due to the significantly strong acidity of TfOH in the PIL.

3.2.2. Autoprotolysis thermodynamics of $DEEAH^+ \cdot TfO^-$

The autoprotolysis enthalpy, ΔH_{AP}°, was determined by calorimetric titration of the basic PIL containing excess DEEA with the acidic PIL containing excess TfOH. Fig. 4 shows the cumulative heat of reaction Σq_r divided by the amount of DEEA n_{DEEA} as a function of the degree of titration, H/B; the added amount of added TfOH divided by that of the initial DEEA. As a result, ΔH_{AP}° = 71.0 kJ/mol was obtained. Interestingly, this value is larger than that in water despite the similar autoprotolysis constant, indicating the entropically favorable autoprotolysis in the PIL. The parameters are summarized in Table 1, where the autoprotolysis Gibbs energy ΔG_{AP}° and the corresponding entropy ΔS_{AP}° were obtained by $\Delta G_{AP}^\circ = -RT \ln K_{AP} = \Delta H_{AP}^\circ - T\Delta S_{AP}^\circ$. In $DEEAH^+ \cdot TfO^-$, ions are converted to neutral molecules through reaction (5a), in which the electrostatic interactions between oppositely charged ions disappear. This situation is opposite in water, where neutral molecules generate ions through reaction (5b) to enhance the solvation structure. Thus, the ΔS_{AP}° value is thus less negative (favorable contribution to autoprotolysis) in the PIL than in water. This trend was observed in EAN; [33] however, the ΔS_{AP}° value is much smaller in $DEEAH^+ \cdot TfO^-$ than that in EAN, indicating that the neutralized DEEA partly acts as a liquid structure maker. Thus, we propose a hydrogen bond formation between

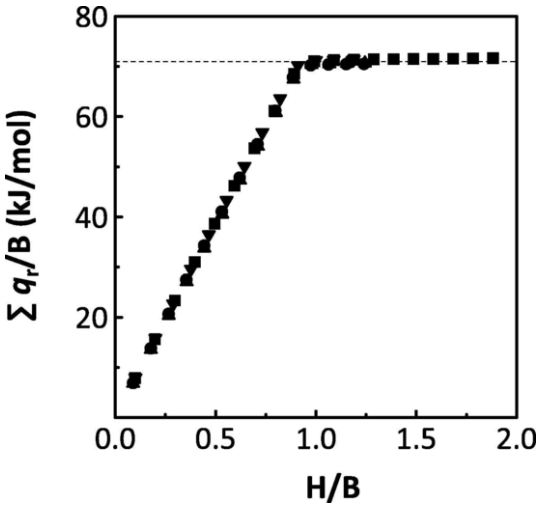

Fig. 4. Calorimetric titration curve of neutralization in $DEEAH^+ \cdot TfO^-$. Basic sample containing DEEA is titrated with an acidic titrant containing TfOH. The cumulative heat of reaction (Σq_r) is divided by the initial amount of DEEA in the sample (B). H/B is the added amount of TfOH divided by B.

Table 1
Thermodynamic parameters of autoprotolysis in the present ionic liquid ($DEEAH^+ \cdot TfO^-$), EAN and water.

	pK_{AP}	ΔG_{AP}°	ΔH_{AP}°	$T\Delta S_{AP}^\circ$	ΔS_{AP}°
		kJ/mol	kJ/mol	kJ/mol	J/mol·K
$DEEAH^+ \cdot TfO^-$	14.9	85.0	71.0	−14.1	−47
EAN [33]	9.83	56.1	81.6	25.5	86
Water [38]	14.0	79.9	55.9	−24.0	−81

DEEA and the ubiquitously existing $DEEAH^+$, as typically shown in Scheme 1. Two $DEEAH^+$ have the ability to form hydrogen bonds between the O of the hydroxyl group and NH^+ of ammonium by nature, whereas the electrostatic repulsion prevents them from approaching each other. Once $DEEAH^+$ is converted to DEEA, it can bridge two $DEEAH^+$ cations through hydrogen bonds to reinforce the solvent structure. This structure was ascertained through DFT calculations (see SI). In contrast, TfO^- has a very weak Lewis basicity and does not contribute to the liquid structure. This situation differs from that in EAN, where both cations and anions are likely to contribute comparably to the liquid structure.[43–47] It should be emphasized that $DEEAH^+ \cdot TfO^-$ and EAN undergo different types of liquid structure changes by acid-base reactions, even though they both belong to protic ionic liquids.

3.3. CNP aggregation in $DEEAH^+ \cdot TfO^-$

3.3.1. CNP ionization equilibrium in $DEEAH^+ \cdot TfO^-$

We previously reported that the ionization equilibrium of pAA on the CNp surface obeys equation (3) in $DEEAH^+ \cdot TfO^-$.[25] Although the equilibrium parameters have then already been obtained ($pK_a^0 = 7.0$ and $\beta = 7.0$), they were redetermined prior to calorimetric titration, in consideration of the batch dependence. In potentiometric titrations, CNp dispersion in the acidic PIL was titrated by the basic PIL containing excess DEEA. Fig. 5(a) and (b) show the results in pH and degree of dissociation (α) as a function of the degree of titration, B/Y; the excess amount of DEEA (added amount of DEEA minus the initial amount of TfOH) divided by the initial amount of Y (B/Y = 1 is the equivalent point). The solution became cloudy when pH reached 8, represented by the blank symbols and a shadowed area, then redispersed when pH was ≈ 11. Using the least-squares procedure, a consistent pK_a^0 and batch dependent β ($pK_a^0 = 7.0$ and $\beta = 4.8$) were obtained. The theoretical curve drawn by a solid line exhibits good agreement with the experimental data, even under flocculation conditions. From this titration, the CNp sample was found to involve 0.021 mol dm^{-3} of Y for 1% Fe_2O_3. This means a smaller carboxylic group density on the CNp surface than that of the previous batch (0.07 mol dm^{-3} for 1% Fe_2O_3). Therefore, the pK_a^{app} value was less sensitive to α, resulting in a decrease in the β value. In contrast, pK_a^0 is independent of Y density. Reasonably, this value reflects the pK_a value of the carboxylic group of pAA at the limit when α approaches zero.

3.3.2. Enthalpy profile of CNp ionization in $DEEAH^+ \cdot TfO^-$

Calorimetric titrations were performed using the same samples used for potentiometric titrations. CNp dispersed stably before (acidic condition) and after (basic condition) titrations, although the sample could not be observed visually during the titration process. Fig. 5(c) shows the titration curves as the apparent molar heat of reaction at each titration point (q_r/n_B) in kJ/mol as a function of B/Y. The solid line exhibits the theoretical curve assuming equations (3) and (4), where the above-mentioned thermodynamic quantities, pK_a^0, β and ΔH_{AP}° are used along with $\Delta H_a^\circ = 30$ kJ/mol, as described after. The experimental data fall on the theoretical line after redispersion (B/Y > 0.65), where pH > 11 and $\alpha > 0.65$. Therefore, the heat of reaction in this region can be clearly assigned to the ionization of the CNp surface pAA. From the least-squares fitting at B/Y > 0.65, the molar ionization enthalpy of Y is determined to be $\Delta H_a^\circ = 30$ kJ/mol (note that the directly observed heat of reaction, 41 kJ/mol, is generated by the reaction HY + DEEA → Y^- + $DEEAH^+$, while ΔH_a° corresponds to HY + TfO^- → Y^- + TfOH). This value resembles the ionization enthalpy of acetic acid in EAN (30.6 kJ/mol),[33] which is clearly larger than that in water, implying no specific behavior in CNp except for acid-base equilibrium in this pH region, however, the value in $DEEAH^+ \cdot TfO^-$ is currently unavailable due to experimental difficulties. Colloidal stability in ionic liquids has been previously proposed to highly depend on a matching between the surface charge density and the size of the solvent ions of ionic liquids.[11] When a good match was achieved at $\alpha = 0.65$, protective surface layers in ionic liquids in the vicinity of charged nanoparticles were formed to stabilize the CNp dispersion.

In contrast, the enthalpic profile before and during flocculation (B/Y < 0.65) exhibited an explicit positive deviation from the theoretical curve. This "extra exotherm" is maximum at the beginning of the titration, then decreases as the titration progresses, and almost disappears at B/Y = 0.65. In an attempt to reproduce the titration pathway, we introduced the second-order term into equation (3), as shown in equation (7). This was applied to pAA in water,[37] however, no improvement was achieved.

$$\mathrm{pH} - \log \frac{\alpha}{1-\alpha} = pK_a^0 + \beta\alpha + \gamma\alpha^2 \quad (7)$$

Thus, we consider that this extra exotherm comes from a change in the solvation of the CNp surface occurring at a small α. When CNps are not charged, they are prevented from aggregation by the steric hindrance of pAA that is swollen in a good solvent thanks to hydrogen bonds, as the main interaction between CNp and the solvent, as well as

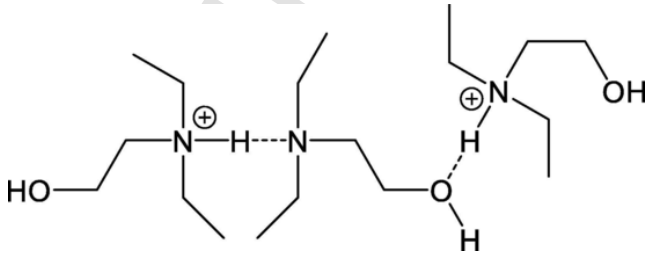

Scheme 1. Possible hydrogen-bond network in $DEEAH^+ \cdot TfO^-$ involving DEEA.

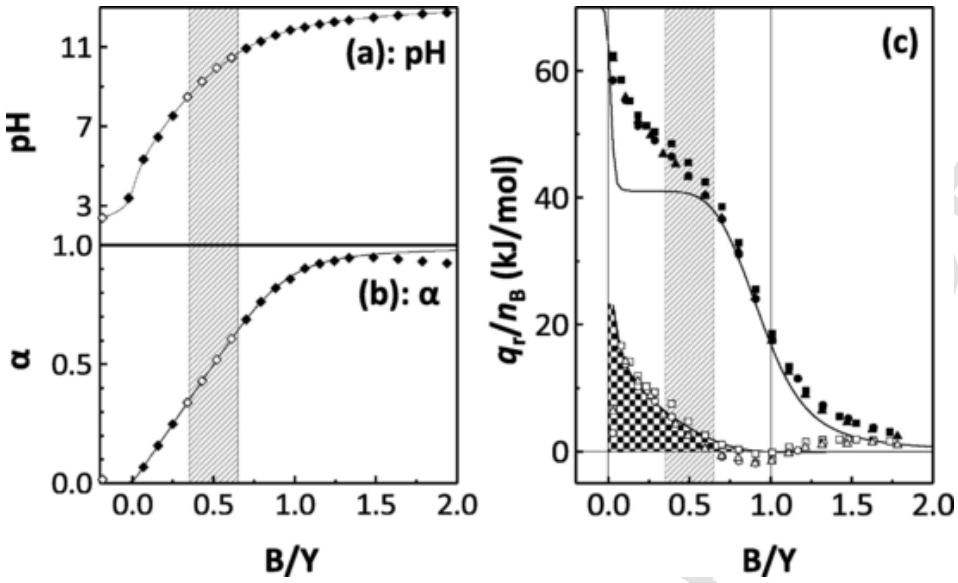

Fig. 5. Potentiometric, (a) and (b), and calorimetric (c) titration curves of pAA-coated γ-Fe_2O_3 nanoparticles dispersed in $DEEAH^+ \cdot TfO^-$ containing excess TfOH, titrated with the basic titrant containing excess DEEA. (a) pH and (b) degree of dissociation (α) plotted against B/Y; the amount of excess DEEA divided by the initial amount of ionizable –COOH in pAA. Blank symbols in (a) and (b) in the shaded region exhibit that the solution is turbid (by eyes). (c) Heats of reaction (q_r) divided by the added amount of DEEA in titrant (n_B) plotted against B/Y. Blank symbols in (c) exhibit the difference between the experimental data (filled symbols) and the theoretical line (calculated by assuming ionization solely, see text). Shaded B/Y range corresponds to that of (a) and (b).

van der Waals forces. Once pAA is ionized, the CNp surface charge increases, enriching the solvent cation, $DEEAH^+$, in the vicinity. In particular, formerly existing hydrogen bonds involving carboxylic groups are replaced by the electrostatic interaction between carboxylate and $DEEAH^+$. These processes could be the reason for the observed extra exotherm. In Fig. 5(c), the deviation between the observed (filled marks) and calculated (solid line) heats of reaction values is plotted using blank symbols. The overall exotherm for this solvent rearrangement can be estimated to be 6 kJ/mol-Y from the area under the blank symbols (filled by sandy pattern). This enthalpic favorability partially explains the smaller pK_a^0 value for CNp than the pK_a value of acetic acid. That is, such a cation-rich environment promotes the ionization of CNp. When B/Y is increased to 0.35, the pAA steric repulsions are no longer sufficient to prevent aggregation and the electrostatic interaction becomes predominant in the CNp solvation layer due to the increased surface charge. However, the charge in this α region is still insufficient to form a good protective and organized solvation layer. In addition, $DEEAH^+$ around the CNp surface possibly tends to bridge negatively charged CNps. As a result, CNp begin to aggregate. According to the previously proposed concept,[11] the matching for stable dispersion between the nanoparticle surface charge density and the sizes of the solvent ions becomes poor. Subsequent calorimetric data did not show any evidence of the release of condensed cations throughout the titration. Therefore, the cations remain close to the negatively charged CNp during aggregation and the explanation formerly presented still holds: the surface of the CNp can be regarded as well swollen by $DEEAH^+$, acting as a bumper to prevent extensive close approach of the CNps.[25] This results in aggregates that are loose enough to facilitate ionization of the inner carboxylic groups during titration. When the CNp surface charge becomes sufficiently large at B/Y = 0.65, the aggregates can redisperse.

4. Conclusion

The acid-base properties of the ionic liquid $DEEAH^+ \cdot TfO^-$ and its origin were elucidated. Interestingly, the autoprotolysis entropy emphasizes the difference between the solvent structure of $DEEAH^+ \cdot TfO^-$ and that of another protic ionic liquid, EAN. Molecular-scopic approaches such as spectroscopic techniques and MD simulations may reinforce this conclusion in the future.

The ionic liquid $DEEAH^+ \cdot TfO^-$ was used to study the mechanism for colloidal stability, using iron oxide nanoparticles coated with a pH-sensitive polymer, pAA. The enthalpy profile corresponding to nanoparticle ionization was quantified for the first time in an ionic liquid and was compared with that in water. The enthalpic contribution was small in the aqueous phase, implying an entropic driving force for CNp aggregation. In contrast, an exotherm was observed in the ionic liquid at a low pH before CNp aggregation. We ascribe this exotherm to the condensation of the solvent cation around CNp. Unlike the case in water, an enthalpic driving force in the subsequent aggregation was found out. This cation-enriched layer remains surrounding CNp even in the flocculation condition. Since the cations are also part of the solvent, the aggregates are regarded as well swollen. At the same time, this solvation layer allows pAA on the CNp surface to be ionized in response to the bulk pH, even inside the aggregate. Aggregates are thus redispersed reversibly at higher pH. When considering ionic liquids as colloidal dispersing media, their dual role as a solvent and as a counterion itself will be the key to the stabilization mechanism. In addition, it is worth noting that calorimetric measurements have proved to be a powerful tool to investigate the invisible phenomena in colloid systems because heats of solvation change were detected in a pH region where no special observation was found by potentiometry. Further investigations are required for other combinations of nanoparticles and ionic liquids.

CRediT authorship contribution statement

Ryo Kanzaki: Conceptualization, Writing – original draft. **Mika Sako:** Investigation. **Hitoshi Kodamatani:** Resources. **Takashi Tomiyasu:** Resources. **Clément Guibert:** Methodology. **Jérôme Fresnais:** Methodology. **Véronique Peyre:** Methodology, Writing – review & editing.

Declaration of Competing Interest

The authors declare that they have no known competing financial interests or personal relationships that could have appeared to influence the work reported in this paper.

Acknowledgements

This work was supported by JSPS KAKENHI Grant Number 21K05115, 19H01168, and 21K18753, and the 47th research grant from The Iwatani Naoji Foundation.

This work was partly supported by Nanotechnology Platform Program (Molecule and Material Synthesis) of the Ministry of Education, Culture, Sports, Science and Technology (MEXT), Japan.

Appendix A. Supplementary material

Supplementary data to this article can be found online at https://doi.org/10.1016/j.molliq.2021.118146.

References

[1] V.P. Walden, Ueber die Molekulargrösse und elektrische Leitfähigkeit einiger geschmolzenen Salze, Bull. Acad. Imp. Sci. (St. Petersburg) 8 (6) (1914) 405–422.
[2] H.H. Ashassi-Sorkhabi, A. Kazempour, Application of Pitzer and six local composition models to correlate the mean ionic activity coefficients of aqueous 1-butyl-3-methylimidazolium bromide ionic liquid solutions obtained by EMF measurements, J. Chem. Thermodyn. 110 (2017) 71.
[3] C. Ma, A. Laaksonen, C. Liu, X. Lu, X. Ji, The peculiar effect of water on ionic liquids and deep eutectic solvents, Chem. Soc. Rev. 47 (2018) 8685.
[4] M. Bešter-Rogač, Ionic Liquids: Simple or Complex Electrolytes? Acta Chim. Slov. 67 (1) (2020) 1–14.
[5] G. Perron, A. Hardy, J.-C. Justice, J.E. Desnoyers, Model System for Concentrated Electrolyte Solutions: Thermodynamic and Transport Properties of Ethylammonium Nitrate in Acetonitrile and in Water, *J. Solution Chem.* 22 (1993) 1159.
[6] M. Allen, D.F. Evans, R. Lumry, Thermodynamic properties of the ethylammonium nitrate + water system: Partial molar volumes, heat capacities, and expansivities, J. Solution Chem. 14 (8) (1985) 549–560.
[7] R. Kanzaki, H. Daiba, H. Kodamatani, T. Tomiyasu, Validation of pH Standards and Estimation of the Activity Coefficients of Hydrogen and Chloride Ions in an Ionic Liquid, Ethylammonium Nitrate, J. Phys. Chem. B 122 (2018) 10593–10599.
[8] R. Kanzaki, S. Uchida, H. Kodamatani, T. Tomiyasu, Copper (II) Chloro Complex Formation Thermodynamics and Structure in Ionic Liquid, 1-Butyl-3-Methylimidazolium Trifluoromethanesulfonate, J. Phys. Chem. B 121 (41) (2017) 9659–9665.
[9] Z. He, P. Alexandridis, Ionic liquid and nanoparticle hybrid systems: Emerging applications, Adv. Colloid Interface Sci. 244 (2017) 54.
[10] Z. He, P. Alexandridis, Nanoparticles in ionic liquids: Interactions and organization, Phys. Chem. Chem. Phys. 17 (2015) 18238.
[11] J.C. Riedl, M.A. Kazemi, F. Cousin, E. Dubois, S. Fantini, S. Lois, R. Perzynski, V. Peyre, Colloidal dispersions of oxide nanoparticles in ionic liquids: elucidating the key parameters, Nanoscale Adv. 2 (4) (2020) 1560–1572.
[12] K. Bhattacharya, M. Sarkar, T.J. Salez, S. Nakamae, G. Demouchy, F. Cousin, E. Dubois, L. Michot, R. Perzynski, V. Peyre, Structural, Thermodiffusive and Thermoelectric Properties of Maghemite Nanoparticles Dispersed in Ethylammonium Nitrate, Chem. Engineer. 4 (2020) 5.
[13] M. Marium, M. Hoque, M.S. Miran, M.L. Thomas, I. Kawamura, K. Ueno, K. Dokko, M. Watanabe*, Rheological and Ionic Transport Properties of Nanocomposite Electrolytes Based on Protic Ionic Liquids and Silica Nanoparticles, Langmuir 36 (2020) 148−158.
[14] E.I. Chereches, J.I. Prado, C. Ibanescu, M. Danu, A.A. Minea, L. Lugo, Viscosity and isobaric specific heat capacity of alumina nanoparticle enhanced ionic liquids: An experimental approach, J. Mol. Liq. 317 (2020).
[15] E.I. Chereches, J.I. Prado, M. Chereches, A.A. Minea, L. Lugo, Experimental study on thermophysical properties of alumina nanoparticle enhanced ionic liquids, J. Mol. Liq. 291 (2019).
[16] P. Priyananda, H. Sabouri, N. Jain, B.S. Hawkett, Steric Stabilization of γ-Fe_2O_3 Superparamagnetic Nanoparticles in a Hydrophobic Ionic Liquid and the Magnetorheological Behavior of the Ferrofluid, Langmuir 34 (2018) 3068.
[17] H. Yang, H. Zhang, J. Peng, Y. Zhang, G. Du, Y. Fang, Smart magnetic ionic liquid-based Pickering emulsions stabilized by amphiphilic Fe_3O_4 nanoparticles: Highly efficient extraction systems for water purification, J. Colloid Interface Sci. 485 (2017) 213.
[18] Y. Zhao, T. Boström, Ionic liquid and nanoparticle based magnetic electrolytes: Design, preparation, and electrochemical stability characterization, J. Mol. Liquids 213 (2016) 268.
[19] M. Mamusa, J. Siricix-Plenet, R. Perzynski, F. Cousin, E. Dubois, V. Peyre, Concentrated assemblies of magnetic nanoparticles in ionic liquids, Faraday Discuss. 181 (2015) 193.
[20] M. Mamusa, J. Siriex-Plénet, F. Cousin, E. Dubois, V. Peyre, Tuning the colloidal stability in ionic liquids by controlling the nanoparticles/liquid interface, Soft Matter 10 (2014) 1097.
[21] M. Mamusa, J. Sirieix-Plénet, F. Cousin, R. Perzynski, E. Dubois, V. Peyre, Microstructure of colloidal dispersions in the ionic liquid ethylammonium nitrate: influence of the nature of the nanoparticles' counterion, J. Phys.: Coondens. Matter 26 (2014) 284113.
[22] L. Rodríguez-Arco, M.T. López-López, F. González-Caballero, J.D.G. Durán, Steric repulsion as a way to achieve the required stability for the preparation of ionic liquid-based ferrofluids, J. Colloid Interface Sci. 357 (2011) 252.
[23] N. Jain, X. Zhang, B.S. Hawkett, G.G. Warr, Stable and water-tolerant ionic liquid ferrofluids, ACS Appl. Mater. Interfaces 3 (3) (2011) 662–667.
[24] C. Guibert, V. Dupuis, J. Fresnais, V. Peyre, Controlling nanoparticles dispersion in ionic liquids by tuning the pH, *J. Colloid Interface Sci.* 454 (2015) 105.
[25] R. Kanzaki, C. Guibert, J. Fresnais, V. Peyre, Dispersion mechanism of polyacrylic acid-coated nanoparticle in protic ionic liquid, N, N-diethylethanolammonium trifluoromethanesulfonate, J. Colloid Interface Sci. 516 (2018) 248–253.
[26] R. Massart, Preparation of Aqueous Magnetic Liquids in Alkaline and Acidic Media, *IEEE Trans. Magn.* 17 (1981) 1247.
[27] J.-C. Bacri, R. Perzynski, D. Salin, V. Cabuil, R. Massart, Magnetic Colloidal Properties of Ionic Ferrofluids, J. Magn. Magn. Mater. 62 (1986) 36.
[28] S. Lefebure, E. Dubois, V. Cabuil, S. Neveu, R. Massart, Monodisperse Magnetic Nanoparticles: Preparation and Dispersion in Water and Oils, J. Mater. Res. 13 (1998) 2975.
[29] J.-F. Berret, O. Sandre, A. Mauger, Size Distribution of Superparamagnetic Particles Determined by Magnetic Sedimentation, Langmuir 23 (2007) 2993.
[30] B. Chanteau, J. Fresnais, J.-F. Berret, Electrosteric Enhanced Stability of Functional Sub-10 nm Cerium and Iron Oxide Particles in Cell Culture Medium, Langmuir 25 (2009) 9064.
[31] A. Sehgal, Y. Lalatonne, J.-F. Berret, M. Morvan, Precipitation-Redispersion of Cerium Oxide Nanoparticles with Poly(acrylic Acid): Toward Stable Dispersions, Langmuir 21 (2005) 9359.
[32] H.A. Flaschka, Edta titrations an introduction to theory and practice, Pergamon Press, Oxford, 1964.
[33] R. Kanzaki, H. Kodamatani, T. Tomiyasu, Proton Thermodynamics in a Protic Ionic Liquid, Ethylammonium Nitrate, Chem. Eur. J. 25 (2019) 13500.
[34] J. Fresnais, M. Yan, J. Courtois, T. Bostelmann, A. Bée, J.-F. Berret, Poly(acrylic acid)-coated iron oxide nanoparticles: Quantitative evaluation of the coating properties and applications for the removal of a pollutant dye, *J. Colloid Interface Sci.* 395 (2013) 24.
[35] I.T. Lucas, S. Durand-Vidal, E. Dubois, J. Chevalet, P. Turq, Surface Charge Density of Maghemite Nanoparticles: Role of Electrostatics in the Proton Exchange, J. Phys. Chem. C 111 (2007) 18568.
[36] K.E. Brahmi, M. Rawiso, J. François, Potentiometric titration of acrylamide-acrylic acid copolymers: Influence of the concentration, Eur. Polym. J. 29 (1993) 1531.
[37] M. Mandel, The potentiometric titration of weak polyacids, *Europ. Polym. J.* 6 (1970) 807.
[38] J.J. Christensen, L.D. Hansen, R.M. Izatt, Handbook of Proton Ionization Heats, John Wiley and Sons, New York, 1976.
[39] V. Crescenzi, F. Quadrifoglio, F. Delben, Calorimetric investigation of poly (methacrylic acid) and poly(acrylic acid) in aqueous solution, J. Polym. Sci. Part A-2: Polym. Phys. 10 (1972) 357.
[40] J. Škerjanc Biophysical Chemistry 1 (1974) 376.
[41] V. Crescenzi, F. Delben, F. Quadrifoglio, D. Dolar, Comparative study of the enthalpy of ionization of polycarboxylic acids in aqueous solution, J. Phys. Chem. 77 (1973) 539.
[42] L. Vitorazi, N. Ould-Moussa, S. Sekar, J. Fresnais, W. Loh, J.P. Chapel, J.F. Berret, Evidence of a two-step process and pathway dependency in the thermodynamics of poly (diallyldimethylammonium chloride)/poly (sodium acrylate) complexation, Soft Matter 10 (47) (2014) 9496–9505.
[43] R. Hayes, S. Imberti, G.G. Warr, R. Atkin, Amphiphilicity Determines Nanostructure in Protic Ionic Liquids, Phys. Chem. Chem. Phys. 13 (2011) 3237.
[44] Y. Umebayashi, W.-L. Chung, T. Mitsugi, S. Fukuda, M. Takeuchi, K. Fujii, T. Takamuku, R. Kanzaki, S. Ishiguro, Liquid Structure and the Ion-Ion Interactions of Ethylammonium Nitrate Ionic Liquid Studied by Large Angle X-Ray Scattering and Molecular Dynamics Simulations, J. Comput. Chem. Jpn. 7 (2008) 125.
[45] X. Song, H. Hamano, B. Minofar, R. Kanzaki, K. Fujii, Y. Kameda, S. Kohara, M. Watanabe, S.I. Ishiguro, Y. Umebayashi, Structural heterogeneity and unique distorted hydrogen bonding in primary ammonium nitrate ionic liquids studied by high-energy X-ray diffraction experiments and MD simulations, J. Phys. Chem. B 116 (9) (2012) 2801–2813.
[46] K. Fumino, A. Wulf, R. Ludwig, Hydrogen Bonding in Protic Ionic Liquids: Reminiscent of Water, *Angew. Chem. Int. Ed.* 48 (2009) 3184.
[47] R. Hayes, I. Silvia, G.G. Warr, R. Atkin, The Nature of Hydrogen Bonding in Protic Ionic Liquids, Angew. Chem. Int. Ed. 52 (2013) 4623.